High-Pressure Transformations and Stability of Ferromagnesite in the Earth's Mantle

Eglantine Boulard, François Guyot, Guillaume Fiquet

HIGH-PRESSURE TRANSFORMATIONS AND STABILITY OF FERROMAGNESITE IN THE EARTH'S MANTLE

Boulard Eglantine[1], Guyot François[1] & Fiquet Guillaume[1]

[1] Sorbonne Université, UMR CNRS 7590, Muséum National d'Histoire Naturelle, IRD, Institut de Minéralogie, Physique des Matériaux et Cosmochimie-IMPMC, 4 Place Jussieu, 75005 Paris, France.

Abstract

Ferromagnesite $(Mg,Fe)CO_3$ plays a key role in the transport and storage of carbon in the deep Earth. Experimental and theoretical studies demonstrated its high stability at high pressure and temperature against melting or decomposition. Several pressure-induced transformations of ferromagnesite have been reported at conditions corresponding to depths greater than ~1100 km in the Earth's lower mantle. Although there is still no consensus on their exact crystallographic structures, evidences are strong of a change in carbon environment from the low-pressure planar CO_3^{2-} ion into carbon atoms tetrahedrally coordinated by four oxygens. High-pressure iron-bearing phases concentrate a large amount of Fe^{3+} as a result of intra-crystalline self-redox reactions. These crystallographic particularities may have significant implications on carbon reservoirs and fluxes in the deep Earth.

Keywords

Carbonates, lower mantle, mineral physics, deep carbon cycle

1 Introduction

Carbon exchange between the Earth's interior and surface occurs over time scales of hundreds millions of years constituting the geodynamical carbon cycle. Surficial carbon is recycled by means of subduction into the deep Earth. Estimations of the carbon flux that reaches the deep Earth in subduction ranges from 0.0001 to 52 megatons of carbon annually (Kelemen & Manning, 2015). This huge uncertainty hinges on poor constraints on the amount of carbon retained by subducting slabs. Carbonate inclusions in diamonds suggest that carbon is transported down to the transition zone depths (Brenker et al., 2007; Kaminsky, 2012; Wang et al., 1996); however, whether any carbon reaches the lower mantle is still controversial. Most subducted carbon is expected to melt and/or breakdown and return to the Earth's surface via volcanism (Kelemen & Manning, 2015; Thomson et al., 2016). However, relatively oxidizing conditions and low slab temperatures may result in the transportation of carbon to greater depths which could feed the core mantle boundary (CMB) (Martirosyan et al., 2015). Yet, a quantitative estimation of carbon or CO_2 released at the core mantle boundary remains unconstrained, as are precise mechanisms for transportation of volatiles to the very deep mantle. In particular, the behaviors of such phases in the presence of deep mantle minerals such as silicates, iron oxides or metallic iron, remain to be evaluated.

Carbon is recycled into the deep mantle in majority as carbonates which mainly occur as calcite $CaCO_3$, dolomite $CaMg(CO_3)_2$, and magnesite $MgCO_3$ at the Earth's surface. Due to chemical reactions with silicates such as pyroxenes and bridgmanite, ferromagnesite $(Mg,Fe)CO_3$ is considered to be the dominant carbonate phase in the deep mantle (e.g. Kushiro et al., 1975; Biellmann et al., 1993). Behavior of ferromagnesite at depth is therefore critical to evaluate the storage capacity and fluxes of carbon. Because of the scarcity of natural samples coming from the lower mantle, knowledge of ferromagnesite's stability and generally of deep processes mainly result from theoretical and experimental studies. The latter requires the ability to reach high pressure and temperature (P-T) conditions of the Earth's mantle and to use micro/nanoscale probes to characterize samples. Laser heated diamond anvil cell is the main static pressure device that is used for studying carbon-bearing phases at the Earth's mantle and core conditions. This technique permits to reach pressures above 300 GPa and temperatures up to 5000 K (e.g. Tateno et al., 2010) by heating with double-sided high-powered infrared lasers available in house and at synchrotron X-ray beamlines. The excellent transparency of single-crystal diamond windows to a wide range of electro-magnetic radiation is compatible with numerous analytical probes for more comprehensive *in situ* characterization of high P-T

behavior. This is critical in the case of non-quenchable phases or dynamic studies where squeeze, cook and look experiments are not sufficient. A detailed review of the different techniques can be found in Mao & Boulard (2013).

In this chapter, we present a review of recent studies dealing with the high-pressure behavior of carbonates on the solid solution join between magnesite and siderite ($FeCO_3$). We first present ferromagnesite high-pressure behaviors and structures as reported in the recent years. We then discuss evidences of particular processes such as the self-redox reactions of Fe-bearing carbonates. Finally we discuss potential implications for the Earth's system.

2 Compression of Mg-Fe Rhombohedral Carbonate

Siderite and magnesite are isomorphous with calcite and crystallize in a rhombohedral symmetry with the R-3c space group (Graf, 1961) (Figure 3.1A). Represented with a hexagonal unit cell, these carbonates contain six formula units per unit cell. They consist of an alternation of layers along the c-axis of cations (Fe^{2+}, Mg^{2+}) in six-fold oxygen coordination and carbon in trigonal planar $(CO_3)^{2-}$ groups. The orientations of two consecutive carbonate ions are staggered relative to each other with the cation at the center of symmetry.

In situ X-ray diffraction (XRD) studies at high pressure show a high stability of calcite structured $MgCO_3$ up to ~80 GPa-2500 K (Fiquet et al., 2002). No evidences of decomposition or melting under P-T conditions down to the core-mantle boundary (CMB) was observed (Dorogokupets, 2007; Fiquet et al., 2002; Gillet, 1993; Solopova et al., 2015). $MgCO_3$ can also be synthesized from the recombination of oxides MgO and CO_2 at mantle P-T conditions (Boulard et al., 2012; Scott et al., 2013). The c-axis is significantly more compressible than the a-axis, attributable to the tight bonding of C-O in CO_3 groups (Katsura et al., 1991). Polyhedral bulk modulus of MgO_6 octahedra was found to be nearly identical to those of $MgCO_3$ (Ross, 1997). However, *in situ* XRD refinements and infrared (IR) spectroscopic analyses showed that at 20 to 50 GPa, C-O bonds expand before contracting (Fiquet et al., 2002; Santillán et al., 2005). This particular behavior produced by the rotation of MgO_6 octahedra likely contributes to the remarkable stability of the R-3c structure in carbonates at high pressure (Fiquet et al., 2002; Santillán et al., 2005).

Fe^{2+} substitution for Mg^{2+} results in a nearly linear increase of the bulk modulus from 103 to 117 GPa (~10%), (Zhang et al., 1998). The same trend has been observed in other ferromagnesian silicates and oxides. This is also observed in silicate spinels, where the bulk modulus increases by ~13 % between Mg_2SiO_4 to Fe_2SiO_4 (Hazen, 1993). At ~50 GPa, iron in Fe-bearing magnesite undergoes a spin transition (Mattila et al., 2007). This isostructural

transition results in an increase in density and compressibility (Lavina et al., 2009), and is expected to affect the partition coefficient of Fe between $(Mg,Fe)CO_3$ and $(Mg,Fe)SiO_3$. As a result, composition of carbonate in equilibrium with Mg-Fe bridgmanite would become closer to siderite at pressures above 50 GPa (Lobanov et al., 2015; Weis et al., 2017). Compared to magnesite, siderite decomposes at lower temperatures (~400° and 500° lower at 1 and 2 GPa, respectively) (Tao et al., 2013). Although the decarbonation boundary of siderite is very close to the average mantle geotherm at about 3 GPa (Tao et al., 2013), typical cold and hot subduction paths are well within the stability fields of both siderite and magnesite.

3 High-pressure polymorphism of ferromagnesite.

High pressure and temperature phase transition in $MgCO_3$ was first demonstrated experimentally by Isshiki et al. (2004) who observed diffraction peaks at 115 GPa-2200 K that could not be assigned to any decomposition products (MgO or CO_2). Transmission electron microscopy (TEM) analyses on the recovered sample showed a homogeneous amorphous sample area rich in Mg, C and O (Irifune et al., 2005). This discovery inspired significant interest in both experimental and theoretical mineral physics. Systematic searches through databases of known crystal structures combined with energy minimization first indicated that a pyroxene structure (space group C2/c) becomes energetically more favorable than magnesite above ~100 GPa (Skorodumova, 2005). Later, Oganov et al. (2006) reported that a $C222_1$ pyroxene-type structure, also predicted in $CaCO_3$, was even more stable. Both structures contain zigzag chains of corner-sharing CO_4^{4-} tetrahedra. It is worth mentioning that USPEX simulations at 110 GPa and 150 GPa also found a number of other low-enthalpy structures that are competitive with these pyroxene structures over a wide pressure range (Oganov et al., 2008).

Pressure-Temperature conditions at which experimental studies reported phase transitions of ferromagnesite are reported in Figure 4.1. There is no consensus about those high-pressure crystallographic structures (Figure 3.1 and Table 4.1) (Boulard et al., 2011, 2012; Cerantola et al., 2017; Isshiki et al., 2004; Liu et al., 2015; Merlini et al., 2015). Those differences might be due to the existence of multiple metastable phases with close free energies and/or to differences in compositions of the starting material.

Concerning the magnesian end-member, Isshiki et al. (2004) proposed an orthorhombic structure above 115 GPa-2200 K (noted Mag-II in Figure 4.1). As no structural refinement could be performed, no atom positions were proposed. In 2011, Boulard et al. reported a transition of magnesite into a monoclinic structure above 80 GPa at 2300 K. Rietveld refinement was not possible but, through comparison with previous theoretical studies (Oganov

et al., 2008), a crystalline structure with a P21/c space group made of groups of three $(CO_4)^{4-}$ tetrahedra sharing one corner that constitute $(C_3O_9)^{6-}$ rings, was proposed (Figure 3.1b). Mg-Fe composition was refined with the same structure (Fe-Mag-II). Non-hydrostatic conditions might have favored metastable phases in those experiments as no pressure medium was used. However, reversal reactions using oxides as starting materials (e.g. $MgO + CO_2$) to maximize synthesis of thermodynamically stable phases rather than metastable intermediate states yielded same structure.

High-pressure studies on pure $FeCO_3$ show the coexistence of rhombohedral siderite with a new structure (Sid-II) above 1400 K at 40 GPa (Boulard et al., 2012; Liu et al., 2015). These two phases co-exist up to about ~70 GPa-2200 K, where room pressure siderite fully disappears. Liu et al. (2015) proposed an orthorhombic unit cell and used the same unit cell for Fe-Mag-II. It is still unclear whether this structure is based on CO_4 groups as no Rietveld refinement were performed. Boulard et al. (2012), reported the recombination of FeO and CO_2 oxides into an $Fe_4C_3O_{12}$ high-pressure phase (Figure 3.1c). Chemical composition was deduced from Electron Energy Loss Spectroscopy (EELS) analyses on the recovered samples following the method developed by Egerton (1996). Due to similitude in terms of chemical composition and unit cell parameters with the olivine-structured Laihunite silicate $(Fe^{3+},Fe^{2+})_2SiO_4$, Boulard et al. (2012) proposed a monoclinic structure with a $P2_1/b$ space group based on isolated $(CO_4)^{4-}$ groups.

More recently, single crystal XRD studies were performed on $(Mg,Fe)CO_3$ (Merlini et al., 2015) and $FeCO_3$ (Cerantola et al., 2017) , allowing structural refinements of crystallographic structures with atom position determination. At pressure above 74 GPa and temperature between 1400 K and 1650 K, Cerantola et al. (2017) observed transformation of $FeCO_3$ into an $Fe_4C_3O_{12}$ high-pressure phase (Sid-II), with an hexagonal structure with R-3c space group formed by isolated CO_4 groups. Up to 2500 K, $Fe_4C_3O_{12}$ coexists with a second high-pressure phase, $Fe_4C_4O_{13}$ (Sid-III), a monoclinic structure with zigzag-shaped $(C_4O_{13})^{10-}$ chains formed by four corner shared CO_4 groups. The same high-pressure structure was reported for ferromagnesite at 135 GPa-2600 K (2900 km) by Merlini et al. (2015).

3.1 Evidence for tetrahedrally coordinated carbon

Identification of CO_4 groups in high-pressure structures based solely on XRD is difficult as it requires precise structural refinements. Moreover, localizing light elements such as carbon is not easy. As mentionned above, only Merlini et al. (2015) and Cerantola et al. (2017) could demonstrate tetrahedrally coordinated carbon from direct single-crystal-XRD measurements in the stoichiometries: $Mg_2Fe_2C_4O_{13}$, $Fe_4C_4O_{13}$ and $Fe_4C_3O_{12}$.

Vibrational spectroscopies, Raman and IR, are also particularly sensitive to carbon chemical environment and permit to probe quite directly C-O bonds. Boulard et al. (2015), reported the first *in situ* characterization of C–O bonds in a post-magnesite phase. They found that after transformation into the Fe-Mag-II, the IR spectrum exhibits unique features not present in the low-pressure spectrum. The band assignment relied on first-principles calculations of the IR spectrum of tetrahedrally coordinated carbon in $MgCO_3$ ($P2_1/a$ space group). A mode at ~1,304 cm^{-1} at ~80 GPa, characteristic of the C-O asymmetric stretching vibration in CO_4 groups, could be used as a fingerprint of CO_4 groups in high-pressure mineral phases. An intense Raman band at ~1,025cm^{-1} (at 105 GPa) with a pressure dependence of ~1.8cm^{-1}/GPa in $P2_1/c$ $CaCO_3$ was recently proposed as characteristic of the symmetrical stretching vibration in its CO_4 groups (Lobanov et al., 2017).

Electron and x-ray spectroscopies at the Carbon K-edge performed on recovered samples also allowed to define signatures associated to tetrahedrally coordinated carbon. Analyses were either collected by EELS using TEM or by synchrotron radiation-based Scanning Transmission X-Ray Microscopy (STXM) coupled to the acquisition of x-ray absorption spectra (XAS). C K-edge on an ambient pressure rhombohedral (R-3c) carbonate sample display peaks at 290.3 and 298.3 eV that can be assigned to 1s → p* electronic transition and one peak at 300.5 eV assigned to 1s → s*, all in carbonate CO_3 groups (Hofer & Golob, 1987; Zhou et al., 2008). Spectra collected on recovered samples transformed into the high-pressure phases of the two compositions $FeCO_3$ and $(Mg,Fe)CO_3$ show different spectroscopic signatures. The main peak is broader and slightly shifted to higher energy (290.47 eV in Fe-Mag-II and 290.67 eV in Sid-II) and a second peak is observed at 287.35 eV in both compositions (Boulard et al., 2012). These spectroscopic signatures are interpreted as a fingerprint of CO_4 groups and the slight energy shift of the main peak between the two compositions may reflect different degrees of polymerization of CO_4 groups. Fe content in the $(Mg,Fe)CO_3$ solid solution likely affects polymerization of CO_4 groups. While isolated $(CO_4)^{4-}$ tetrahedra are reported in pure Fe composition, high-pressure polymorphs of Mg-rich carbonates are based on polymerized CO_4 groups, i.e. $(C_3O_9)^{6-}$ or $(C_4O_{13})^{10-}$ chains (see Arapan et al., 2007; Boulard et al., 2011; Cerantola et al., 2017; Isshiki et al., 2004; Merlini et al., 2015; Oganov et al., 2008; Panero & Kabbes, 2008)

3.2 Self-redox reactions in Fe^{2+}-bearing carbonates

Another particularity of the crystal chemistry of ferromagnesite and siderite's high-pressure structures is the preferential association of the CO_4 tetrahedral groups with trivalent iron.

Incorporation of trivalent iron or of mixed 3+/2+ valences with high Fe^{3+} contents in these phases was inferred from the stoichiometries (Boulard et al. 2011; 2012; Cerantola et al., 2017; Merlini et al., 2015). Fe $L_{2,3}$-edges spectra collected *ex situ* by EELS or STXM on the recovered samples from the high-pressure phases of $FeCO_3$ or $(Mg,Fe)CO_3$ confirmed high Fe^{3+} contents in the products of transformation at high-pressure (Boulard et al. 2012). The redox counterpart for Fe^{3+} formation could eventually be the stabilization of Fe^0 as observed in silicates in the case of the disproportionation reaction of bridgmanite (Frost & McCammon, 2008). However, Fe^0 has never been identified in samples resulting from the transformation of Fe^{2+}-bearing carbonates at high pressure. Starting from exclusively Fe^{2+} bearing carbonates, formation of Fe^{3+} is instead balanced by partial reduction of carbon-bearing molecular groups (CO_3^{2-} or CO_2) (Table 4.2). We call this a self-redox process since Fe^{2+} and CO_3^{2-} initially present in the low pressure compound react with each other to yield Fe^{3+} and reduced carbon species (C or CO). Indeed, diamond coexisting with high-pressure transformation products of Fe^{2+}-bearing carbonates or Fe^{2+}-bearing oxides in presence of CO_2 was reported by Boulard et al. (2011) and Boulard et al. (2012). Coexisting Fe^{3+}-bearing iron oxides have also been reported such as magnetite or hematite and their associated high-pressure structures (Boulard et al., 2011, 2012; Cerantola et al., 2017), as well as newly described iron oxides Fe_5O_7 (Cerantola et al., 2017) and $Fe_{13}O_{19}$ (Merlini et al., 2015). Decomposition of $FeCO_3$ into Fe_3O_4 + C was also reported in the stability field of classical CO_3^{2-}-bearing carbonates (<50 GPa) (Boulard et al., 2012; Cerantola et al., 2017). In these low-pressure experiments, only partial decomposition took place, as carbonate remained present even after heating up to one hour. The possible existence of a thermodynamic boundary of siderite decomposition remains to be further investigated. Overall, current available data suggest that the stability of high-pressure phases containing CO_4 groups enhances the dismutation of Fe^{2+}-bearing carbonates into Fe^{3+}-bearing phases and reduced carbon species such as diamond.

Conclusions and outlooks

Ferromagnesite $(Mg,Fe)CO_3$ or close stoichiometries containing oxidized carbon species are very stable under extreme P-T conditions. The phase diagram of the Mg-Fe-C-O system is very rich and yields several compounds containing CO_4 groups enriched in Fe^{3+}even though only Fe^{2+} was the iron speciation of iron in the starting materials. As SiO_4 groups in silicates, CO_4 groups are present as isolated or polymerized.

This high-pressure change in carbon environment may have significant implications on carbon reservoirs and fluxes. At upper mantle conditions, CO_3^{2-}-bearing melts differ from

silicate melts as they exhibit ultra-low viscosity potentially resulting in high mobilities (Kono et al., 2014). Due to the capacity of CO_4^{4-} to polymerize, the viscosity of CO_4-bearing melts is expected to be significantly higher (Oganov et al., 2013). This would inhibit mobility of CO_4-bearing melts in the lower mantle and might stabilize deep carbon reservoirs. The systematic presence of trivalent iron in the Fe-rich CO_4-bearing structures also suggests that other compositions could be stabilized, such as aluminum-rich compositions which do not exist in association with carbon at ambient conditions (Merlini et al., 2015).

These newly described high-pressure structures derived from ferromagnesite represent potential oxidized carbon carriers into the lowermost mantle. Whether these phases remain stable in subducting slab or in regular mantle lithologies is still uncertain. In a recent study, Boulard et al., (2018) reported that deep carbon and hydrogen cycles may be more interconnected than previously thought as $Fe_4C_3O_{12}$ replaces pyrite-structured FeO_2H_x in presence of CO_2. This reaction provides a new mechanism for hydrogen release as H_2O within the deep mantle. However, as highlighted by Dorfman et al., (2018), ferromagnesite and the associated high-pressure structures are sensitive to redox breakdown. Ferromagnesite reacts with metallic iron in the lower mantle to form either diamond or carbide, depending on the availability of metallic iron. If this is the case, calcite, which is less sensitive to redox breakdown, could be revived as an interesting oxidized carbon carrier at large depth in the mantle. More oxidizing conditions like those prevailing in subducting slabs may still stabilize ferromagnesite and related stoichiometries. The redox stabilities of calcite, ferromagnesite, and of their high-pressure transformation products remain to be extensively tested as a function of T, P and fO_2.

A next step will obviously be to consider the Fe-Mg-C-O high-pressure phase diagram in the context of a silicate-rich lithology. Recent studies on $CaCO_3$ and $MgCO_3$ in presence of an excess of SiO_2 or $MgSiO_3$ show that $CaCO_3$ is likely to undergo decomposition into CO_2 and Ca-perovskite under any slab P-T conditions, while $MgCO_3$ may be preserved under a very cold slab P-T conditions (Kakizawa et al., 2015; Maeda et al., 2017; Seto et al., 2008; Takafuji et al., 2006; Zhang et al., 2018). However none of these studies have considered iron-rich compositions, which, deserve special attention due to the effect of the iron spin transition and of self-redox processes with oxidized carbon species. There is increasing evidence that such self-redox processes might let strong imprint in actual processes. For example, self-redox reaction of ferromagnesite was recently observed in a natural sample of shocked carbonate at the Xiuyan impact crater (Chen et al., 2018). Whether it is related to impact-induced formation of CO_4 groups or not will deserve further studies. Self-redox processes might also provide an

interesting explanation of some of the carbonate inclusions in deep diamonds (Boulard et al., 2011).

References

Arapan, S., Souza de Almeida, J., & Ahuja, R. (2007). Formation of sp3 Hybridized Bonds and Stability of CaCO3 at Very High Pressure. *Physical Review Letters*, *98*, 268501. https://doi.org/10.1103/PhysRevLett.98.268501

Biellmann, C., Gillet, P., Guyot, F., Peyronneau, J., & Reynard, B. (1993). Experimental evidence for carbonate stability in the Earth's lower mantle. *Earth and Planetary Science Letters*, *118*(1–4), 31–41. https://doi.org/10.1016/0012-821X(93)90157-5

Boulard, E., Gloter, A., Corgne, A., Antonangeli, D., Auzende, A., Perrillat, J.-P., et al. (2011). New host for carbon in the deep Earth. *Proceedings of the National Academy of Sciences of the United States of America*, *108*(13), 5184–5187. https://doi.org/10.1073/pnas.1016934108/-/DCSupplemental.www.pnas.org/cgi/doi/10.1073/pnas.1016934108

Boulard, E., Menguy, N., Auzende, a.-L., Benzerara, K., Bureau, H., Antonangeli, D., et al. (2012). Experimental investigation of the stability of Fe-rich carbonates in the lower mantle. *Journal of Geophysical Research*, *117*(B2), B02208. https://doi.org/10.1029/2011JB008733

Boulard, E., Pan, D., Galli, G., Liu, Z., & Mao, W. L. (2015). Tetrahedrally coordinated carbonates in Earth 's lower mantle. *Nature Communications*, *6*, 6311. https://doi.org/10.1038/ncomms7311

Boulard, E., Guyot, F., Menguy, N., Corgne, A., Auzende, A., Perrillat, J., & Fiquet, G. (2018). CO2-induced destabilization of pyrite-structured FeO2Hx in the lower mantle. *National Science Review*, *0*, 1–8. https://doi.org/10.1093/nsr/nwy032

Brenker, F. E., Vollmer, C., Vincze, L., Vekemans, B., Szymanski, A., Janssens, K., et al. (2007). Carbonates from the lower part of transition zone or even the lower mantle. *Earth and Planetary Science Letters*, *260*(1–2), 1–9. https://doi.org/10.1016/j.epsl.2007.02.038

Cerantola, V., Bykova, E., Kupenko, I., Merlini, M., Ismailova, L., McCammon, C., et al. (2017). Stability of iron-bearing carbonates in the deep Earth's interior. *Nature Communications*, *8*(May), 15960. https://doi.org/10.1038/ncomms15960

Chen, M., Shu, J., Xie, X., Tan, D., & Mao, H. (2018). Natural diamond formation by self-redox of ferromagnesian carbonate. *Proceedings of the National Academy of Sciences*,

115(11), 2676–2680. https://doi.org/10.1073/pnas.1720619115

Dorfman, S. M., Badro, J., Nabiei, F., Prakapenka, V. B., Cantoni, M., & Gillet, P. (2018). Carbonate stability in the reduced lower mantle. *Earth and Planetary Science Letters*, *489*, 84–91. https://doi.org/10.1016/j.epsl.2018.02.035

Dorogokupets, P. I. (2007). Equation of state of magnesite for the conditions of the Earth's lower mantle. *Geochemistry International*, *45*(6), 561–568. https://doi.org/10.1134/S0016702907060043

Egerton, R. F. (1996). *Electron Energy-Loss Spectroscopy in the Electron Microscope* (2nd ed.). New York: Press Plenum.

Fiquet, G., Guyot, F., Kunz, M., Matas, J., Andrault, D., & Hanfland, M. (2002). Structural refinements of magnesite at very high pressure. *American Mineralogist*, *87*, 1261–1265. https://doi.org/10.2138/am-2002-8-927

Frost, D. J., & McCammon, C. A. (2008). The Redox State of Earth's Mantle. *Annual Review of Earth and Planetary Sciences*, *36*, 389–420. https://doi.org/10.1146/annurev.earth.36.031207.124322

Gillet, P. (1993). Stability of magnesite (MgCO3) at mantle pressure and temperature conditions : A Raman spectroscopic study. *American Mineralogist*, *78*, 1328–1331.

Graf, D. L. (1961). Crystallographic tables for the rhombohedral carbonates. *American Mineralogist*, *46*, 1283–1316.

Hazen, R. M. (1993). Comparative Compressibilities of Silicate Spinels: Anomalous Behavior of (Mg,Fe)2SiO4. *Science (New York, N.Y.)*, *259*(5092), 206–209. https://doi.org/10.1126/science.259.5092.206

Hofer, F., & Golob, P. (1987). short note new examples for near-edge fine structures in electron energy loss spectroscopy Ferdinand HOFER and Peter GOLOB, *21*, 379–383.

Irifune, T., Isshiki, M., & Sakamoto, S. (2005). Transmission electron microscope observation of the high-pressure form of magnesite retrieved from laser heated diamond anvil cell. *Earth and Planetary Science Letters*, *239*(1–2), 98–105. https://doi.org/10.1016/j.epsl.2005.05.043

Isshiki, M., Irifune, T., Hirose, K., Ono, S., Ohishi, Y., Watanuld, T., et al. (2004). Stability of magnesite and its high-pressure form in the lowermost mantle. *Nature*, *427*(January), 60–63. https://doi.org/10.1029/2000C000736

Kakizawa, S., Inoue, T., Suenami, H., & Kikegawa, T. (2015). Decarbonation and melting in $MgCO_3$–SiO_2 system at high temperature and high pressure. *Journal of Mineralogical and Petrological Sciences*, *110*(4), 179–188. https://doi.org/10.2465/jmps.150124

Kaminsky, F. (2012). Mineralogy of the lower mantle: A review of "super-deep" mineral inclusions in diamond. *Earth-Science Reviews*, *110*, 127–147. https://doi.org/10.1016/j.earscirev.2011.10.005

Katsura, T., Tsuchida, Y., Ito, E., Yagi, T., Utsumi, W., & Akimoto, S. (1991). Stability of Magnesite under the Lower Mantle Conditions. *Proceedings of the Japan Academy. Ser. B: Physical and Biological Sciences*, *67*(4), 57–60. https://doi.org/10.2183/pjab.67.57

Kelemen, P. B., & Manning, C. E. (2015). Reevaluating carbon fluxes in subduction zones, what goes down, mostly comes up. *Proceedings of the National Academy of Sciences*, *112*(30), E3997–E4006. https://doi.org/10.1073/pnas.1507889112

Kono, Y., Kenney-Benson, C., Hummer, D., Ohfuji, H., Park, C., Shen, G., et al. (2014). Ultralow viscosity of carbonate melts at high pressures. *Nature Communications*, *5*, 1–8. https://doi.org/10.1038/ncomms6091

Lavina, B., Dera, P., Downs, R. T., Prakapenka, V., Rivers, M., Sutton, S., & Nicol, M. (2009). Siderite at lower mantle conditions and the effects of the pressure-induced spin-pairing transition. *Geophysical Research Letters*, *36*(23), L23306. https://doi.org/10.1029/2009GL039652

Liu, J., Lin, J.-F., & Prakapenka, V. B. (2015). High-Pressure Orthorhombic Ferromagnesite as a potential deep-mantle carbon carrier. *Scientific Reports*, *5*, 7640. https://doi.org/10.1038/srep07640

Lobanov, S. S., Goncharov, A. F., & Litasov, K. D. (2015). Optical properties of siderite (FeCO3) across the spin transition: Crossover to iron-rich carbonates in the lower mantle. *American Mineralogist*, *100*(5–6), 1059–1064. https://doi.org/10.2138/am-2015-5053

Lobanov, S. S., Dong, X., Martirosyan, N. S., Samtsevich, A. I., Stevanovic, V., Gavryushkin, P. N., et al. (2017). Raman spectroscopy and x-ray diffraction of sp3-CaCO3 at lower mantle pressures. *Physical Review B*, *96*, 104101. https://doi.org/10.1103/PhysRevB.96.104101

Maeda, F., Ohtani, E., Kamada, S., Sakamaki, T., Hirao, N., & Ohishi, Y. (2017). Diamond formation in the deep lower mantle: a high-pressure reaction of MgCO3 and SiO2. *Scientific Reports*, *7*(January), 40602. https://doi.org/10.1038/srep40602

Mao, W. L., & Boulard, E. (2013). Nanoprobes for Deep Carbon. *Reviews in Mineralogy and Geochemistry*, *75*(1), 423–448. https://doi.org/10.2138/rmg.2013.75.13

Martirosyan, N. S., Litasov, K. D., Shatskiy, A. F., & Ohtani, E. (2015). Reactions of iron with calcium carbonate at 6 GPa and 1273-1873 K: Implications for carbonate reduction in the deep mantle. *Russian Geology and Geophysics*, *56*(9), 1322–1331.

https://doi.org/10.1016/j.rgg.2015.08.008

Mattila, a, Pylkkänen, T., Rueff, J.-P., Huotari, S., Vankó, G., Hanfland, M., et al. (2007). Pressure induced magnetic transition in siderite FeCO3 studied by x-ray emission spectroscopy. *Journal of Physics: Condensed Matter*, *19*(38), 386206. https://doi.org/10.1088/0953-8984/19/38/386206

Merlini, M., Hanfland, M., Salamat, A., Petitgirard, S., & Müller, H. (2015). The crystal structures of Mg2Fe2C4O13 with tetrahedrally coordinated carbon, and Fe13O19, synthesized at deep mantle conditions. *American Mineralogist*, *100*, 2001–2004. https://doi.org/10.1524/zkri.219.10.621.50817

Oganov, A. R., Glass, C. W., & Ono, S. (2006). High-pressure phases of CaCO3: Crystal structure prediction and experiment. *Earth and Planetary Science Letters*, *241*(1–2), 95–103. https://doi.org/10.1016/j.epsl.2005.10.014

Oganov, A. R., Ono, S., Ma, Y., Glass, C. W., & Garcia, A. (2008). Novel high-pressure structures of MgCO3, CaCO3 and CO2 and their role in Earth's lower mantle. *Earth and Planetary Science Letters*, *273*, 38–47. https://doi.org/10.1016/j.epsl.2008.06.005

Oganov, A. R., Hemley, R. J., Hazen, R. M., & Jones, A. P. (2013). Structure, Bonding, and Mineralogy of Carbon at Extreme Conditions. *Reviews in Mineralogy and Geochemistry*, *75*(1), 47–77. https://doi.org/10.2138/rmg.2013.75.3

Panero, W. R., & Kabbes, J. E. (2008). Mantle-wide sequestration of carbon in silicates and the structure of magnesite II. *Geophysical Research Letters*, *35*(14), 1–5. https://doi.org/10.1029/2008GL034442

Ross, N. L. (1997). The equation of state and high-pressure behavior of magnesite. *American Mineralogist*, *82*, 682–688.

Santillán, J., Catalli, K., & Williams, Q. (2005). An infrared study of carbon-oxygen bonding in magnesite to 60 GPa. *American Mineralogist*, *90*(10), 1669–1673. https://doi.org/10.2138/am.2005.1703

Scott, H. P., Doczy, V. M., Frank, M. R., Hasan, M., Lin, J.-F., & Yang, J. (2013). Magnesite formation from MgO and CO2 at the pressures and temperatures of Earth's mantle. *American Mineralogist*, *98*(7), 1211–1218. https://doi.org/10.2138/am.2013.4260

Seto, Y., Hamane, D., Nagai, T., & Fujino, K. (2008). Fate of carbonates within oceanic plates subducted to the lower mantle , and a possible mechanism of diamond formation. *Physics and Chemistry of Minerals*, *35*, 223–229. https://doi.org/10.1007/s00269-008-0215-9

Skorodumova, N. V. (2005). Stability of the MgCO3 structures under lower mantle conditions. *American Mineralogist*, *90*, 1008–1011. https://doi.org/10.2138/am.2005.1685

Solopova, N. A., Dubrovinsky, L., Spivak, A. V., Litvin, Y. A., & Dubrovinskaia, N. (2015). Melting and decomposition of MgCOinf3/inf at pressures up to 84 GPa. *Physics and Chemistry of Minerals*, *42*(1), 73–81. https://doi.org/10.1007/s00269-014-0701-1

Takafuji, N., Fujino, K., Nagai, T., Seto, Y., & Hamane, D. (2006). Decarbonation reaction of magnesite in subducting slabs at the lower mantle. *Physics and Chemistry of Minerals*, *33*(10), 651–654. https://doi.org/10.1007/s00269-006-0119-5

Tao, R., Fei, Y., & Zhang, L. (2013). Experimental determination of siderite stability at high pressure. *American Mineralogist*, *98*, 1565–1572. https://doi.org/10.2138/am.2013.4351

Tateno, S., Hirose, K., Ohishi, Y., & Tatsumi, Y. (2010). The Structure of Iron in Earth's Inner Core. *Science*, *330*, 359–361. https://doi.org/10.1126/science.1194662

Thomson, A. R., Walter, M. J., Kohn, S. C., & Brooker, R. A. (2016). Slab melting as a barrier to deep carbon subduction. *Nature*, *529*(7584), 76–79. https://doi.org/10.1038/nature16174

Wang, A., Pasteris, J. D., Meyer, H. O. A., & Dele-duboi, M. L. (1996). Magnesite-bearing inclusion assemblage in natural diamond, *141*, 293–306.

Weis, C., Sternemann, C., Cerantola, V., Sahle, C. J., Spiekermann, G., Harder, M., et al. (2017). Pressure driven spin transition in siderite and magnesiosiderite single crystals. *Scientific Reports*, *7*(1), 1–10. https://doi.org/10.1038/s41598-017-16733-3

Wood, B. J., Pawley, A., & Frost, D. R. (1996). Water and carbon in the Earth's mantle. *Philosophical Transactions of the Royal Society of London*, *354*, 1495–1511.

Zhang, J., Martinez, I., Guyot, F., & Reeder, R. J. (1998). Effects of Mg-Fe 2+ substitution in calcite-structure carbonates : Thermoelastic properties. *American Mineralogist*, *83*, 280–287.

Zhang, Z., Mao, Z., Liu, X., Zhang, Y., & Brodholt, J. (2018). Stability and Reactions of CaCO 3 Polymorphs in the Earth's Deep Mantle. *Journal of Geophysical Research: Solid Earth*, *123*(8), 6491–6500. https://doi.org/10.1029/2018JB015654

Zhou, D., Metzler, R. A., Tyliszczak, T., Guo, J., Abrecht, M., Coppersmith, S. N., & Gilbert, P. U. P. A. (2008). Assignment of polarization-dependent peaks in carbon K-edge spectra from biogenic and geologic aragonite. *Journal of Physical Chemistry B*, *112*(41), 13128–13135. https://doi.org/10.1021/jp803176z

Table 4.1

	Theoretical Calculations:	P range (GPa)	Space Group	a	b	c	β
$MgCO_3$	Skorodumova et al., 2005	>113	C2/c				
	Oganov et al., 2006	>107	$C222_1$	5.552	7.201	2.880	
	Oganov et al., 2008	82-138	C2/m	8.094	6.488	6.879	103.98
		138-160	$P2_1$	4.534	7.792	5.086	104.54
	Experimental Studies Starting material						
$MgCO_3$	Isshiki et al., 2004 $Mg_{0.994}Ca_{0.006}CO_3$	>115	Ortho.	7.18	5.03	4.47	
	Boulard et al., 2011 $Mg_{0.997}Fe_{0.003}CO_3$	>80	P21/c	8.37	6.37	6.80	104.57
$Mg_2Fe_2(C_4O_{13})$	Merlini et al., 2015 $Mg_{0.26}Fe_{0.7}Mn_{0.025}Ca_{0.015}CO_3$	135	Mono.	9.822	3.902	13.154	108.02
$Mg_{0.25}Fe_{0.3}(C_3O_9)_{0.233}$	Boulard et al., 2011 $Mg_{0.249}Fe_{0.748}Mn_{0.005}Ca_{0.006}CO_3$	>80	P21/c	7.83	6.37	6.73	101.97
$Fe_4C_4O_{13}$	Cerantola et al., 2017 $FeCO_3$	>74	C12/c 1	10.261	3.985	13.455	107.85
$Fe_4C_3O_{12}$	Cerantola et al., 2017 $FeCO_3$	>74	R3c	12.762	12.762	5.332	
$Fe_4C_3O_{12}$	Boulard et al., 2012 $FeO+CO_2$	>50	Mono.	10.16	6.66	6.15	93.04
$FeCO_3$	Liu et al., 2015 $Fe_{0.998}Mn_{0.002}CO_3$ $Mg_{0.33}Fe_{0.65}Mn_{0.2}CO_3$	>50	Pmm2	10.99	6.34	5.27	

Table 4.2

	Reference	Chemical Reaction
R1	Merlini et al., 2015	$93Fe_{0.7}Mg_{0.3}CO_3 = 20Mg_{1.395}Fe_{2.605}(C_4O_{13}) + Fe_{13}O_{19} + 13C$
R2	Boulard et al., 2011	$20Mg_{0.25}Fe_{0.75}CO_3 = 20Mg_{0.25}Fe_{0.3}(C_3O_9)_{0.233} + 3Fe_3O_4 + 6CO$ (or $3C + CO_2$)
R3	Boulard et al., 2012	$4FeO + 4CO_2 \rightarrow Fe_4C_3O_{12} + C$
R4	Boulard et al., 2012	$4FeO + 5CO_2 = Fe_4C_3O_{12} + 2CO$
R5	Boulard et al., 2012	$2Fe_2O_3 + 3CO_2 = Fe_4C_3O_{12}$
R6	Cerantola et al., 2017	$4FeCO_3 = Fe_4C_3O_{12} + C$
R7	Cerantola et al., 2017	$7Fe_4C_3O_{12} + 3C = 6Fe_4C_4O_{13} + 2Fe_2O_3$
R8	Cerantola et al., 2017	$8Fe_4C_3O_{12} = 6Fe_4C_4O_{13} + 4Fe_2O_3 + 3O_2$

Figure Captions:

Figure 3.1

Crystallographic structures of Mg-Fe carbonates as reported in the literature. a) the calcite-type rhombohedral structure in which Mg-Fe carbonates crystallize at ambient conditions, b) high-pressure structure of magnesite and ferromagnesite ($MgCO_3$ and $Mg_{0.25}Fe_{0.3}(C_3O_9)_{0.233}$) Boulard et al., 2011, c) high-pressure phase of siderite: $Fe_4C_3O_{12}$ Boulard et al., 2012, d) $Fe_4C_3O_{12}$ Cerantola et al., 2017, $Fe_4C_4O_{13}$ and $Mg_2Fe_2(C_4O_{13})$ Cerantola et al., 2017 and Merlini et al., 2015. White and grey spheres are oxygens and Fe/Mg cations respectively, and black triangle or black tetrahedra are carbon polyhedral.

Figure 4.1

Experimental ferromagnesite phase diagram. Mag-I, Sid-I and Fe-Mag-I refers to ambient magnesite, siderite and ferromagnesite structures, and phases II and III to the associated high-pressure polymorphs.

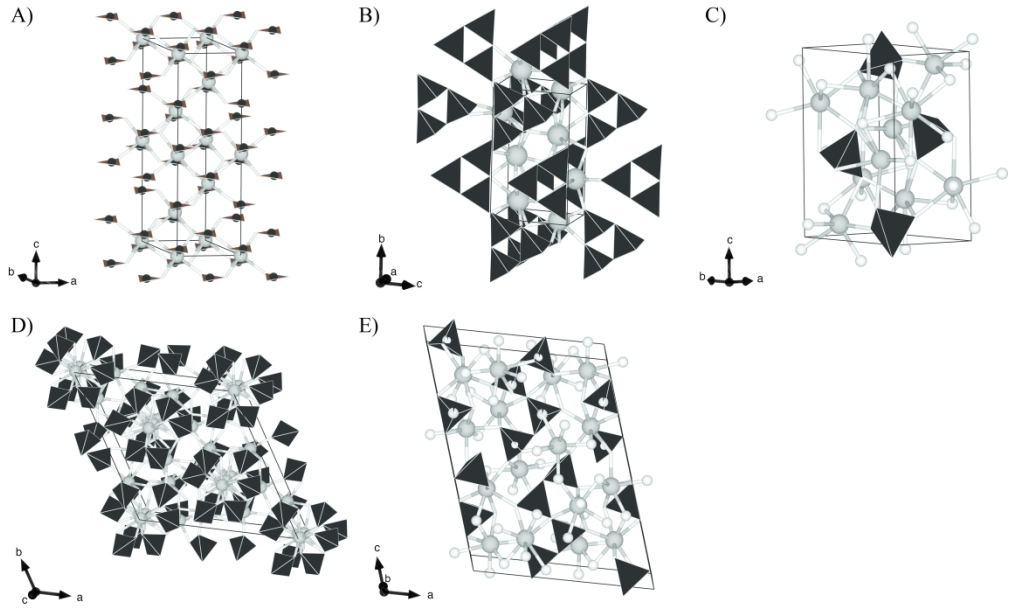

Figure 3.1
Crystallographic structures of Mg-Fe carbonates as reported in the literature. a) the calcite-type rhombohedral structure in which Mg-Fe carbonates crystallize at ambient conditions, b) high-pressure structure of magnesite and ferromagnesite (MgCO3 and Mg0.25Fe0.3(C3O9)0.233) Boulard et al., 2011, c) high-pressure phase of siderite: Fe4C3O12 Boulard et al., 2012, d) Fe4C3O12 Cerantola et al., 2017, Fe4C4O13 and Mg2Fe2(C4O13) Cerantola et al., 2017 and Merlini et al., 2015. White and grey spheres are oxygens and Fe/Mg cations respectively, and black triangle or black tetrahedra are carbon polyhedral.

511x308mm (300 x 300 DPI)

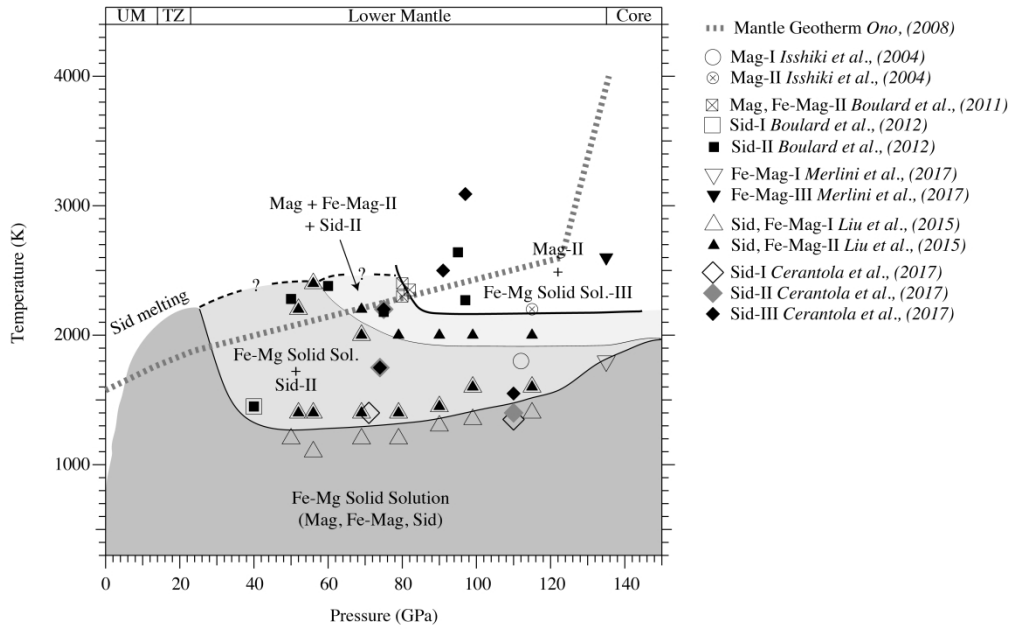

Figure 4.1
Experimental ferromagnesite phase diagram. Mag-I, Sid-I and Fe-Mag-I refers to ambient magnesite, siderite and ferromagnesite structures, and phases II and III to the associated high-pressure polymorphs.

351x218mm (300 x 300 DPI)